JASAE
Journal of Applied Science and Advanced Engineering
Vol. 4 No.1 (2026) ; p. 16 - 21

e-ISSN: 2985-7252
https://jasae.org/

Aerodynamic Performance of the NACA 0012 Airfoil: Lift and Drag Characteristic Across a Range of Angles of Attack

Dedy Septiawan[1*], Dwi Yuliaji[1], and Roy Waluyo[1]
[1]Department of Mechanical Engineering, Universitas Ibn Khaldun Bogor
*e-mail: dedyuuki@gmail.com

ARTICLE HISTORY
Received: 11 September 2025
Revised: 04 November 2025
Accepted: 28 March 2026

KEYWORDS
Lift
Drag
NACA 0012
CFD Simulation

ABSTRACT– The wing is one of the most critical components in an aircraft structure, as it directly contributes to the generation of lift, which enables flight. Without wings, an aircraft would be unable to produce lift or counter aerodynamic drag effectively. This study aims to analyze the lift and drag forces acting on a NACA 0012 airfoil under varying angles of attack and flow velocities. Two approaches were employed: numerical simulations using ANSYS Fluent to investigate airflow patterns and pressure distribution on the upper and lower surfaces of the airfoil, and experimental testing in a wind tunnel to validate and complement the findings. The experiments considered angles of attack of 0°, 3°, 6°, and 9°, with freestream velocities of 1 m/s and 3 m/s. The quantitative data collected include lift coefficient (CL), drag coefficient (CD), the relationships between CL–α, CD–α, and CL–CD, as well as pressure and velocity distributions from the CFD simulations. Both computational and experimental results indicate that increasing the angle of attack produces a significant change in the lift and drag characteristics of the airfoil. In conclusion, variations in the angle of attack have a substantial impact on the aerodynamic flow behavior around the airfoil and on the magnitude of the resulting lift and drag forces.

© Septiawan et. al.

This is an Open Access article distributed under the terms of the Creative Commons CC-BY-4.0 License, which permits unrestricted use, distribution, and reproduction in any medium, provided the original work is properly cited.

Introduction

Aerodynamic performance is a fundamental aspect in the design and development of various transportation and energy systems, such as aircraft, racing vehicles, wind turbines, and drones. One of the key elements in these systems is the airfoil, which is the cross-sectional shape of a wing or surface designed to generate lift when air flows over it [1]. The efficiency of an airfoil is highly influenced by the angle of attack and airflow velocity, which directly determine the magnitude of aerodynamic forces such as lift and drag.

One of the most widely used airfoils in experimental and simulation studies is the NACA 0012, a symmetric airfoil with a maximum thickness of 12% of the chord length [2]. This airfoil exhibits neutral behavior at zero angle of attack due to its symmetric pressure distribution between the upper and lower surfaces. However, when the angle of attack increases, a pressure difference develops between the two surfaces, generating lift. The response of the NACA 0012 to changes in angle of attack makes it an ideal model for understanding flow dynamics in symmetric airfoils, including critical phenomena such as flow separation and stall [3].

During the take-off phase, fixed-wing aircraft generally achieve lift-off at an angle of attack of approximately 12°, which enables the wings to generate sufficient lift as the speed approaches Vy (best rate-of-climb speed). The increase in angle of attack directly increases the lift coefficient until the wings can produce enough lift to overcome the aircraft's weight. After leaving the ground effect, the aircraft experiences an increase in induced drag, thus requiring an additional increase in angle of attack to maintain the same lift [4]. Therefore, managing the angle of attack during the initial climb phase is crucial to ensure that the aircraft can safely maintain climb speed (Vy or Vx).

In the landing phase, the aircraft approaches touchdown with a higher angle of attack, or with a standard approach typically around 10°–12°, depending on flap configuration. This allows the aircraft to maintain stable flight at low speed while remaining well below the stall angle (generally around 15°–18°). The angle of attack (α) is defined as the angle between the airfoil's chord line and the direction of the free-stream airflow. Within a small angle range, an increase in α typically results in a linear increase in lift. However, beyond a certain point, the airflow over the upper surface of the airfoil begins to separate, leading to a sharp decrease in lift and a significant increase in drag. This condition is known as a stall, which can cause a loss of aerodynamic stability and efficiency [5].

To understand the characteristics of airflow around an airfoil and how aerodynamic forces are generated, two primary approaches are commonly used: physical experiments in a wind tunnel and numerical simulations using

Computational Fluid Dynamics (CFD). Wind tunnel testing enables direct observation of airflow and visualization of phenomena such as flow separation through smoke flow techniques. At the same time, CFD provides detailed numerical and visual data on pressure, velocity, and force distribution [6].

This study aims to quantitatively and qualitatively analyze how variations in angle of attack and flow velocity affect the lift and drag forces on the NACA 0012 airfoil. The study employs two main approaches: numerical simulation using CFD with ANSYS Fluent, and physical experimentation using a subsonic wind tunnel. The range of angles of attack analyzed includes 0°, 3°, 6°, and 9°, with airflow velocities of 1 m/s and 3 m/s.

The results of this study are expected to contribute to the fundamental understanding of the aerodynamic performance of symmetric airfoils, as well as provide recommendations for optimal operating angles in applications such as light aircraft, UAVs, or other aerodynamic systems operating at low to moderate speeds. Furthermore, these findings serve as validation data for the development of more complex CFD numerical models in future research.

Material and Methods

A. Aerodynamic Theory Basics

Lift Force (F_L) and drag force (F_D) on an airfoil are generally calculated using the following equations:

$$F_L = \frac{1}{2}\rho v^2 C_L A$$

$$F_D = \frac{1}{2}\rho v^2 C_D A$$

Wherever:

- ρ : air density (kg/m³)
- v : airflow velocity (m/s)
- A : reference surface area
- C_L: lift coefficient
- C_D : drag coefficient

The relationship $F \propto v^2$ explains that aerodynamic forces increase quadratically with velocity. The angle of attack influences the values of C_L and C_D, and an increase in angle of attack within certain limits will enhance lift force before stall occurs.

B. Airfoil

The term airfoil refers to the geometric shape of the cross-sectional area found in various aerodynamic structures such as wings, rotors, propellers, and turbines. The orientation of an airfoil relative to the incoming airflow plays a crucial role in determining its ability to generate lift and drag forces [7]. The forces acting on a body moving through a fluid can be categorized into two main components: lift and drag. The aerodynamic force F on a moving body can be resolved into the drag force D, which is parallel to the incoming flow, and the lift force L, which is perpendicular to the incoming flow, as shown in Figure 1.

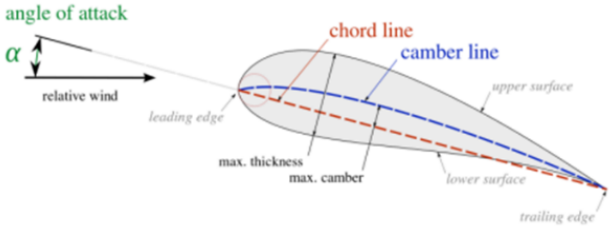

Figure 1. Airfoil nomenclature

The parts of an airfoil can be described as follows:

- Leading edge: the foremost point of an airfoil.
- Trailing edge: the rearmost point of an airfoil.
- Camber line: the line that equally divides the upper and lower surfaces of the airfoil, also referred to as the mean camber line.
- Chord line: the straight line connecting the leading edge and the trailing edge.
- Chord: the distance between the leading edge and the trailing edge.
- Maximum camber: the most significant distance between the mean camber line and the chord line, measured from the leading edge as a percentage of the chord.
- Maximum thickness: the most significant distance between the upper and lower surfaces of the airfoil, measured perpendicular to the chord line [8].

C. Airfoil NACA 0012

The NACA 0012 airfoil is a symmetric profile commonly used as a baseline in aerodynamic studies. Due to its symmetry, this airfoil does not generate lift at zero angle of attack [9]. However, its linear response to changes in angle of attack makes it ideal for preliminary studies of aerodynamic characteristics.

D. Wind Tunnel

A wind tunnel is an experimental device used to study airflow behavior around objects [10]. In this study, an open-circuit subsonic wind tunnel was utilized to visualize the flow (smoke flow) and indirectly measure aerodynamic forces through flow patterns.

E. Reynolds Number

The Reynolds number is a dimensionless quantity that is related to ρ (density), v (velocity), L (MAC length or mean aerodynamic chord), and μ (dynamic viscosity). The Reynolds number can be used to determine the type of flow, whether it is laminar or turbulent. If the Reynolds number is 2300, the flow is classified as laminar; however, if the Reynolds number exceeds 4000, the flow is classified as turbulent [11].

F. CFD (Computational Fluid Dynamics)

CFD enables the analysis of fluid flow behavior around objects by numerically solving the Navier-Stokes equations. ANSYS Fluent was used as the primary software in this simulation. The advantage of CFD lies in its capability to visualize detailed distributions of pressure, velocity, and turbulence around the airfoil. In general, there are three main stages in conducting a CFD simulation [12].

- **Preprocessing**

This is the first stage, involving the construction and preparation of the CFD model. It includes defining the geometry, generating the mesh to divide the computational domain into appropriate grids, and specifying the physical parameters such as boundary conditions and fluid properties.

- **Processing or Solving**

At this stage, the defined conditions from preprocessing are calculated using numerical approaches such as finite element, finite difference, or finite volume methods. The solver iterates the calculations until the solution converges.

- **Postprocessing**

The final stage is organizing and interpreting the CFD results, typically in the form of contour plots, graphs, and animations.

G. CFD Simulation

- Implementation Site: Ansys Student 2024 R1 Software on a Personal Computer.
- Software: ANSYS (Fluent)
- Geometry Model: NACA 0012 (chord length = 10 cm)
- Medium: Air flow inkompresibel, subsonik, steady state
- Mesh: Fine mesh around the airfoil with boundary layer mesh
- Boundary Condition: Velocity inlet, pressure outlet, no-slip wall
- Turbulence Model: k-ω SST (to resolve flow separation)
- Variation Parameters:
- Angle of Attact: 0°, 3°, 6°, 9°.
- Velocity: 1 m/s and 3 m/s.

H. Wind Tunnel Experiment

- Wind Tunnel Type: Open-circuit subsonic (size 1.0 m × 0.3 m)
- Instrument: Smoke generator, DSLR camera, anemometer
- Purpose: Flow visualization to detect separation zones, wake regions, and vortices.
- Procedure: Each angle of attack was tested at two different velocities and recorded using smoke flow visualization for flow interpretation.

Results and Discussion

A. Aerodynamics Force Data.

Analysis:

- Effect of Velocity: An increase in force occurs up to ±9× increase to 3×, in line with v2v^2v2.
- Effect of Angle of Attack: Lift increases linearly up to 6°, then the rate of increase slows at 9°, which also shows a significant rise in drag — an early indication of stall.

Maximum Efficiency: The highest L/D ratio occurs at a 6° angle of attack — ideal for optimal aerodynamic performance.

B. CFD and Wind Tunnel Visualization.

The CFD simulation provides a clear visual representation of the changes in pressure distribution and airflow patterns around the NACA 0012 airfoil for each angle of attack variation [13]. The following figures present the static pressure contours and streamlines generated from numerical simulations using ANSYS Fluent.

- **Angle of Attack 0°**

Based on the computational simulation results, the airflow over the NACA 0012 airfoil at an angle of attack of 0° shows a relatively symmetrical flow pattern between the upper and lower surfaces of the profile, as shown in Figure 2. Due to the symmetric shape of the airfoil, the velocity distribution over the upper and lower surfaces is nearly identical. However, the velocity on the upper side tends to be slightly higher due to the curvature effect.

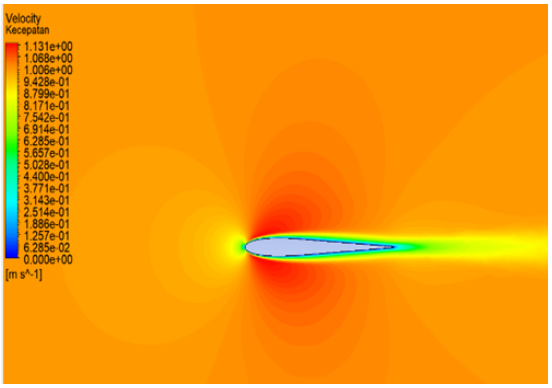

Figure 2. Visualization NACA 0012 AOA 1°

- **Angle of Attack 3°**

Based on the Computational Fluid Dynamics (CFD) simulation, the airflow over the NACA 0012 airfoil at an angle of attack of 3° and a velocity of 1 m/s begins to exhibit asymmetry between the upper and lower surfaces. At the leading edge, the flow

divides between both surfaces; however, due to the positive angle of attack, the airflow over the upper surface travels a longer path compared to the lower surface. This difference in path length causes the velocity on the upper surface to increase while the velocity on the lower surface remains relatively lower. According to Bernoulli's principle, the higher velocity over the upper surface results in reduced static pressure, whereas the lower surface maintains higher pressure due to slower airflow.

- **Angle of Attack 6°**

At an angle of 6°, a sharp pressure gradient develops on the upper surface of the airfoil. The pressure near the leading edge drops significantly, resulting in accelerated airflow over the surface. The streamlines still indicate attached flow, although the wake at the trailing edge begins to widen. This represents the most aerodynamically efficient condition, with the highest lift-to-drag ratio.

- **Angle of Attack 9°**

An angle of attack of 9° shows early indications of stall. Flow separation occurs near the rear portion of the upper surface of the airfoil, indicated by vortex formation and an enlarged wake. The pressure on the upper surface is no longer evenly distributed, and the streamlines begin to show signs of flow detachment. This explains the significant increase in drag and the reduction in aerodynamic efficiency.

C. Results of Average Velocity and Pressure Distribution with Respect to Angle of Attack 1 m/s using CFD are shown in Figures 3 and 4.

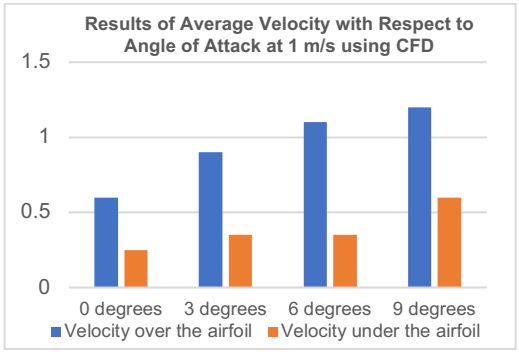

Figure 3. Results Average Velocity Refer to Variation AOA

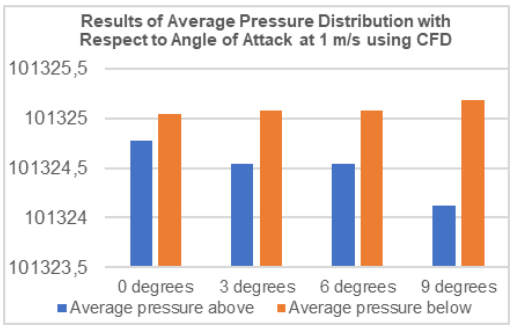

Figure 4. Results Average Pressure Refer of Variation AOA

- **Velocity Distribution Analysis.**

The airflow over the upper surface is consistently faster than over the lower surface. At $\alpha = 0°$, the upper velocity is 1.2 m/s vs. 0.55 m/s lower, with the difference increasing up to 2.3 m/s at $\alpha = 9°$. This confirms that higher angles of attack intensify flow acceleration on the upper surface.

- **Pressure Distribution Analysis**

As predicted by Bernoulli's principle, upper-surface pressure is lower than the lower surface, with differences rising from 1.066 Pa ($\alpha = 0°$) to 7.532 Pa ($\alpha = 9°$). The lower pressure remains nearly constant at ~101,325 Pa, while the upper surface pressure decreases progressively, producing lift.

- **Angle Optimization**

The 6° angle shows strong aerodynamic efficiency, while higher angles approach stall. Within the test range, $\alpha = 9°$ yields maximum lift, but in practice, the optimal angle is typically between 6° and 9° to balance lift and drag.

D. Results of CFD Calculation for the Lift Coefficient and Drag Coefficient with Variables Angle of Attack and Flow Velocity are shown in Table 1.

Table 1. Lift Coefficient and Drag Coefficient with Variables

No	Angle of attack (˚)	Velocity (m/s)	C_L	C_D
1	0	1	0.00015	0.00301
		3	0.00010	0.00155
2	3	1	0.00244	0.00214
		3	0.00284	0.00141
3	6	1	0.00486	0.00229
		3	0.00561	0.00162
4	9	1	0.00693	0.00261
		3	0.00712	0.00182

- **Aerodynamic Dynamics of a Symmetrical Airfoil**

Data at 0°, 3°, and 6° angles of attack show patterns consistent with symmetrical airfoil characteristics. At 0°, the lift coefficient (CL) should approach zero, yet recorded values were 0.00015 and 0.00010 at 1 m/s and 3 m/s, respectively. This may indicate a slight asymmetry in the airfoil geometry or minor experimental errors in angle calibration.

- **Aerodynamic Performance Optimization**

At 6° angle of attack, the airfoil demonstrates optimal performance with CL = 0.0056 and CD = 0.0016, producing the highest lift-to-drag ratio. This condition reflects maximum aerodynamic efficiency, where lift increase remains balanced with proportional drag.

- **Performance Degradation and Stall Phenomena**

At 9°, data show an unusual increase in CL accompanied by an unexpected drop in CD at 1 m/s (0.00301). This anomaly is likely due to experimental error rather than an actual stall, as stall typically involves a sharp CL decrease and CD increase. At 3 m/s, results align better with aerodynamic theory, with CD = 0.00155.

- **Flow Velocity Variation Analysis**

At the exact angle of attack, both CL and CD are consistently higher at 3 m/s than at 1 m/s, in line with aerodynamic theory where lift and drag scale with velocity squared. Lift-to-drag efficiency is also generally higher at 3 m/s, indicating improved overall aerodynamic performance.

- **Relevance in Modern Aviation**

In commercial aviation, optimizing the angle of attack is key for efficiency. Aircraft such as the Airbus A350 and Boeing 787 leverage this to maintain ideal lift-to-drag ratios during cruise, achieving up to 20% fuel savings. Stall analysis has also driven safety innovations, with advanced systems (e.g., Boeing 787) predicting stall conditions 5–8 seconds in advance and applying automatic control corrections, greatly enhancing flight safety.

- **Aerodynamic Dynamics Analysis on a Symmetrical Airfoil**

The characteristics of the symmetrical airfoil at a neutral angle (0°) are shown by a stable lift coefficient (CL) value of around 7.93, reflecting the nature of a symmetrical airfoil that does not generate significant lift without an angle of attack. When the angle of attack is increased to 3°, a drastic change occurs in the aerodynamic characteristics, where CL experiences an exponential jump or a variable change of 171% to 21.49.

- **Optimization of Aerodynamic Performance at an Angle of Attack of 6°**

The data analysis results indicate that an angle of attack of 6° represents the optimal point of aerodynamic performance, with the lift coefficient (CL) reaching 33.92 and the drag coefficient (CD) recorded at 2.16. This condition yields a lift-to-drag (L/D) ratio of 15.7, which is the highest value within the testing range, indicating peak aerodynamic efficiency.

- **Stall Phenomenon and Performance Degradation at an Angle of Attack of 9°**

The data analysis reveals an evident stall phenomenon at an angle of attack of 9°, characterized by a sharp increase in the drag coefficient (CD) by 136% compared to the optimal condition at 6°. This indicates an exponential rise in drag, while the increase in the lift coefficient (CL) is limited to only 14.6%, suggesting that additional lift is not effectively generated.

- **Analysis of Flow Velocity Variations**

From the matrix analysis results on velocity variations, it can be explained that within the tested range of 1–3 m/s, the lift coefficient (CL) shows very minimal changes (less than 0.3%), indicating high stability against velocity fluctuations. Similarly, the drag coefficient (CD) only varies by less than 1.5%.

- **Relevance of Aerodynamic Studies in the Modern Aviation Industry**

In the operational context of commercial aircraft, knowledge of the optimal angle of attack is key to efficiency, where the Airbus A350 and Boeing 787 apply these findings in wing design to maintain an ideal lift-to-drag ratio during the cruise phase, resulting in up to 20% fuel savings compared to previous generations.

Conclusion

From the above discussion, it can be concluded that the Comparative Study between Experimental and Simulation Results of the Flow Patterns around the NACA 0012 Airfoil is as follows:

Changes in angle of attack greatly influence airflow, lift, and drag. Lift increases up to about 6° with best efficiency, but drag also rises, and beyond 10°–12°, stall may occur, so a balance between lift and safety is essential. At 0°, simulations show symmetrical flow with negligible lift and minimal drag. As the angle increases, faster airflow over the upper surface creates pressure differences that generate lift. Wind tunnel tests confirm similar results: at 0°, no lift is produced due to symmetric pressure, while higher angles cause flow acceleration over the upper surface, reduced pressure, and lift formation in line with Bernoulli's principle.

References

[1] D. Singh, R. H. Gajghat, and M. K. Manik, "Experimental Investigation To Examine The Effect Of Shape And Size Of Dimples At Suction Surface Of Aerofoil," vol. 8, no. 12, 2019.

[2] A. Mahato, R. Kant Singh, R. Barnwal, and S. Chandra Rana, "Aerodynamic characteristics of NACA 0012 vs. NACA 4418 airfoil for wind turbine applications through CFD simulation," *Materials Today: Proceedings*, p. S2214785323030754, May 2023, doi: 10.1016/j.matpr.2023.05.439.

[3] R. R. Leknys, M. Arjomandi, R. M. Kelso, and C. H. Birzer, "Dynamic Stall Flow Structure and Forces on Symmetrical Airfoils at High Angles of Attack and Rotation Rates," *Journal of Fluids Engineering*, vol. 141, no. 5, p. 051104, May 2019, doi: 10.1115/1.4041523.

[4] K. Abu Salem, G. Palaia, M. R. Chiarelli, and M. Bianchi, "A Simulation Framework for Aircraft Take-Off Considering Ground Effect Aerodynamics in Conceptual Design," *Aerospace*, vol. 10, no. 5, p. 459, May 2023, doi: 10.3390/aerospace10050459.

[5] T. C. Corke and F. O. Thomas, "Dynamic Stall in Pitching Airfoils: Aerodynamic Damping and Compressibility Effects," *Annu. Rev. Fluid Mech.*, vol. 47, no. 1, pp. 479–505, Jan. 2015, doi: 10.1146/annurev-fluid-010814-013632.

[6] T. Glatzel *et al.*, "Computational fluid dynamics (CFD) software tools for microfluidic applications – A case study," *Computers & Fluids*, vol. 37, no. 3, pp. 218–235, Mar. 2008, doi: 10.1016/j.compfluid.2007.07.014.

[7] M. Albers and W. Schröder, "Lower drag and higher lift for turbulent airfoil flow by moving surfaces," *International Journal of Heat and Fluid Flow*, vol. 88, p. 108770, Apr. 2021, doi: 10.1016/j.ijheatfluidflow.2020.108770.

[8] V. Motta, A. Guardone, and G. Quaranta, "Influence of airfoil thickness on unsteady aerodynamic loads on pitching airfoils," *J. Fluid Mech.*, vol. 774, pp. 460–487, July 2015, doi: 10.1017/jfm.2015.280.

[9] M. R. Ahmed and S. D. Sharma, "An investigation on the aerodynamics of a symmetrical airfoil in ground effect," *Experimental Thermal and Fluid Science*, vol. 29, no. 6, pp. 633–647, July 2005, doi: 10.1016/j.expthermflusci.2004.09.001.

[10] M. Ohba, K. Irie, and T. Kurabuchi, "Study on airflow characteristics inside and outside a cross-ventilation model, and ventilation flow rates using wind tunnel experiments," *Journal of Wind Engineering and Industrial Aerodynamics*, vol. 89, no. 14–15, pp. 1513–1524, Dec. 2001, doi: 10.1016/S0167-6105(01)00130-1.

[11] V. Uruba, "Reynolds number in laminar flows and in turbulence," presented at the 38TH MEETING OF DEPARTMENTS OF FLUID MECHANICS AND THERMODYNAMICS, Liptovsky Mikulas, Slovakia, 2019, p. 020003. doi: 10.1063/1.5114728.

[12] B. Blocken and C. Gualtieri, "Ten iterative steps for model development and evaluation applied to Computational Fluid Dynamics for Environmental Fluid Mechanics," *Environmental Modelling & Software*, vol. 33, pp. 1–22, July 2012, doi: 10.1016/j.envsoft.2012.02.001.

[13] M. Y. Zakaria, M. M. Ibrahim, S. Ragab, and M. R. Hajj, "A computational study of vortex shedding from a NACA-0012 airfoil at high angles of attack," *IJAD*, vol. 6, no. 1, p. 1, 2018, doi: 10.1504/IJAD.2018.089779.